J Ther Eng, Vol. 9, No. 2, pp. 414–428, March 2023

Journal of Thermal Engineering
Web page info: https://jten.yildiz.edu.tr
DOI: 10.18186/thermal.1285134

Journal of Thermal Engineering

Research Article

A CFD investigation of flow separation in an elliptical and circular Ranque-Hilsch vortex tube

Nitin BAGRE[1], Ashok PAREKH[1], Vimal PATEL[1*]

[1]*Department of Mechanical Engineering, Sardar Vallabhbhai National Institute of Technology Surat, 395007, India*

ARTICLE INFO

Article history
Received: 04 October 2021
Accepted: 09 Febuary 2022

Keywords:
Elliptical Vortex Tube; 3D Numerical Investigation; Energy Separation; Constant Area

ABSTRACT

The present work investigates the flow physics inside an elliptical vortex tube. Two different 3D (three-dimensional) domains of circular and elliptical vortex tubes with four nozzles are studied. The cross-sectional area and length of the vortex tube are constant for both of its shape. The pressure at the inlet is 320 kPa for both the shapes and air as a working fluid. Standard k- ε turbulence model is used to predict the flow physics and temperature separation effect inside the tubes. The experimental and numerical findings of earlier researchers provide as validation for the present results. The deviation of the results is found within the permissible limit. The temperature separation phenomenon in an elliptical tube at various cold mass fractions is discussed. The range of cold mass fraction is 0.1 to 0.9. This work also examines the fluid characteristics and flow parameters by tracing the fluid particles within the tube. Fluid characteristics such as static pressure, density, total temperature, static temperature are evaluated. Also, the flow parameters like velocity magnitude, turbulent kinetic energy, axial velocity, and swirl velocity are discussed at the various radial locations inside the tube to get the flow pattern information. It's an attempt to determine the feasible flow mechanism inside an elliptical vortex tube. The comparison between the circular vortex tube and the elliptical vortex tube has been done based on various fluid characteristics and temperature separation. It is found that energy separation is elevated in an elliptical tube by 49.89% at the hot end tube at 0.2 cold mass fraction whereas it is low for cold temperature separation as compared to the circular vortex.

Cite this article as: Nitin B, Ashok P, Vimal P. A CFD investigation of flowseparation in an elliptical and circular Ranque-Hilschvortex tube. J Ther Eng 2023;9(2):424–438.

INTRODUCTION

An eco-friendly device that utilizes the coarctate air to discrete hot and cold streams is named as Ranque-Hilsch Vortex tube. A vortex tube was invented by a French physicist Ranque in 1937. Further, it was modified by a German scientist named Hilsch in 1947; therefore, it is called as Ranque-Hilsch Vortex tube (RHVT). It engenders

***Corresponding author.**
*E-mail address: ds18me008@med.svnit.ac.in

This paper was recommended for publication in revised form by Editor Assoc.Prof Dr. Erman Aslan

the cooling and heating effects simultaneously without using any chemical or refrigerant which urges various industrial applications. It has a fixed structure with motionless parts. The different parts of the vortex tube are vortex generator, vortex chamber, hot tube, and flow regulating valve. The coarctate air enters tangentially through a high-pressure compressor into the vortex chamber via a vortex generator, which generates swirling flow. The process of temperature separation occurs in which the hot stream moves towards the peripheral of the hot end and rest reverses in the opposite direction near the cold exit. The cold exit is positioned nearer to the inlet of the vortex tube. Due to its design and compactness, it's always been keen of interest to the researchers. The advantages of vortex tube are low cost, eco-friendly, compact, lightweight, adjustable temperature range and reliable. Various engineering applications such as for precooling air in liquefying plants, the cooling of airborne electronic equipments. It is also used for cooling of soldered parts and in spot welding. A study by Markal et al. [1] on valve angle, which concluded that the impact of the valve is less compared with the L/D ratio. Kirmaci and Uluer [2] had thoroughly discussed the influence of variables like cold mass fraction (μ_c), number of nozzles, and various inlet pressure conditions on RHVT. Kirmaci et al. [3] used various operating fluids like argon, oxygen, nitrogen, and air and performed exergy analysis. Rafiee and Sadeghiazad [4] evaluated the effects of throttle valve angles. Gutak [5] provided a fairly thorough explanation of the significance of vortex tubes and their use in industrial applications. It was discovered that a vortex tube can be used in a plant pipeline for both heating and cooling purposes in an industry like the natural gas station. An experiment made by Li et al. [6] obtained the stagnation point location in a vortex tube. A wide range of cold fractions has been considered i.e 0.27, 0.63, 0.8, and 0.91. The maximum static temperature is found at the core and it is lower at the peripheral wall. Furthermore, if the cold mass fraction increases or the inlet pressure decreases the stagnation point will move towards the cold region. A hybrid cooling drying system was designed using a vortex tube by Senturk Acar and Arslan [7]. When the work was evaluated using R-134a as the working fluid, it was discovered that in the hot summer, COP and exergy efficiency were 0.0347 and 0.0094, respectively, while in the cold winter, they were 0.0409 and 0.0079. NouriBorujerdi et al. [8] conducted a parametric analysis in which variables such as the quantity of nozzles, the ratio of length to diameter (L/D), and the ratio of the vortex generator were examined. The study found that, when compared to the number of nozzles, the L/D ratio significantly influenced performance. Yadav et al. [9] a vortex tube which has two cold outlets in which, the influence of various outlet shapes over its performance was investigated. The temperature separation effect had been thoroughly discussed by the numerical method and experimental analysis by Westley [10]. Kurosaka [11] explained the acoustic effect which defined the temperature separation effects from the cold outlet to the hot outlet. An optimization methods ANN (Artificial neural network) adopted by Uluer et al.[12] to evaluate the optimum number of nozzles and pressure at the inlet on the performance of the vortex tube. An algebraic stress model (ASM) was adopted to simulated the turbulence in a vortex tube by Eiamsaard and Promvonge [13]. Alhborn and Gordon[14] discussed the various flow zones , along with the secondary circulation inside the tube. The effects of nozzle number were investigated by Behera [15] through numerical and experimental analysis. Aljuwayhel et al. [16] performed a numerical study using RNG and Standard k-ε model to get the understanding of the flow mechanism inside the vortex tube. A comparative study among the CFD analysis and experimental results was made by Skye et al. [17] to calculate the temperature values at the outlets. An Large Eddy Simulation (LES) method to get the details about the temperature fields inside the tube was utilized by Farouk and Farouk [18] which explained the presence low swirl flow at the core of the tube that concurred with low temperature region. Xue et al.[19] examined parameters like pressure elevation, circulation and turbulence of air inside the tube. The inlet pressure plays an important role on the performance of the vortex tube and was well discussed by Rahimi et al. [20]. Pourmahmoud et al. [21] conducted a study to examine the impact of cold orifice diameter on the functionality of the vortex tube. The study found that an ideal cold opening diameter of 4 mm might produce the best cooling benefits. Neeraj Agrawal et al. [22] analysed the performance of vortex tube by admitting different working fluids like air, CO_2 and N_2. It was observed that CO_2 was more effective than the rest of the gases used. The COP for different L/D ratios had also been evaluated. It determined that the highest COP of 0.13 was achieved at L/D ratio 17.5 for 80% μ_c. Adib Bazgir and Nader Nabhani [23] used three different shapes i.e. straight, convergent, and divergent tube to obtain the flow mechanism inside the tube. Rafiee and Sadeghiazad [24] a comparative analysis for various types of vortex tube (RHVT, Parallel VT and Double-Circuit VT) according to their temperature separation magnitude. It is found that the highest temperature separation can be generated through a double circuit VT when compared with RHVT and Parallel VT. The 3D models were created to study the influence of various shapes on the performance of the vortex tube. It was determined that the COP and η (efficiency) of the system can be enhanced with a divergent hot tube. Masoud Rahimi et al. [25] explored the effects of a divergent hot exit angle of the tube. A CFD approach was opted to study the effect of various divergent angles i.e. 1^o,2^o,3^o,4^o and 6^o to analyze the flow physics using vortex tube. Results concluded that the performance of the tube can be increased by optimizing the divergent angle. An experimental and CFD work by Rafiee et al. [26] to investigate the convergent angle of the vortex tube, the convergent angle adopted in

the study was 1-9°. The result concluded that the maximum temperature separation was found at 5°. Also, the cooling rate is increased by 32.03% and heating rate increased by 26.21%. The work also covers the area in which the cold orifice diameter was optimized which found that a 9 mm diameter achieved higher effectiveness. Convergentdivergent vortex tubes can increase the cooling rate, according to Lizan and Ramzi's numerical and experimental examination of them [27]. Masoud Bovand et al. [28] chose a RNG k-ε method to analyze the influence of curvature on the performance of a vortex tube. A twin pipe RHVT was used by Adib Bazgir et al. [29] to examine the impact on cooling rate.According to the study, a cooled hot tube with four nozzles and an L/D ratio of 47.5 can be used to achieve higher temperature separation.Thakare and Parekh [30] describe the use of vortex tubes in industrial applications. The findings indicate that a vortex tube made of PA6 material can enhance its performance. At a 4 bar inlet pressure situation, the cooling rate increased by 10.47% when compared to mild steel. The fundamentals of heat and mass transfer in a flow fluid was well described by Reddy and Sreedevi [31]–[35]. Also, the effect of thermal radiation and chemical reaction on MHD has been explained by Reddy et al. [36], [37]. A study on the flow and heat transfer on stretchable disk was illustrated by Reddy et al. [38]. It is cleared from the past investigation that the core aim of the researchers is to enhance the performance of vortex tube by modifying the design and also by considering the various materials. So, on the basis of previous studies the present study deals with the temperature separation and flow physics inside an elliptical vortex tube which is not reported previously. The present study also compared a circular vortex tube with an elliptical vortex tube on the basis of temperature separation.

Table 1. Computational domain details

S.No.	Parameters	Dimensions
1.	Length of the tube ($L_{vortextube}$)	133 mm
2.	Inlet diameters (D_{inlet})	10 mm
3.	Height of the nozzle (H_{nozzle})	9 mm
4.	Width of the nozzle (w_{nozzle})	2mm
5.	Cold orifice diameter (D_{cold})	5 mm
6.	Area of the tube ($A_{hot\ tube}$)	63.61 mm^2

Objective of The Present Study

Studying the flow physics and temperature separation effect in an elliptical vortex tube is the main objective of the current work. The influence of shape over its performance were also analyzed. It is evident from the past investigation that the shape of the vortex tube has a great influence on its performance. Here, for the first time, an elliptical shape vortex tube has been presented to get an understanding of temperature separation. The past investigation also shows that the cooling rate can be enhanced by changing the shape of a circular vortex tube. Hence, an elliptical-shaped vortex tube is introduced and analyzed.

GEOMETRICAL MODEL

The present numerical work has been carried out using same dimension of vortex tube reported by Ouadha et al. [39]. The circular shape was modified by an elliptical shape

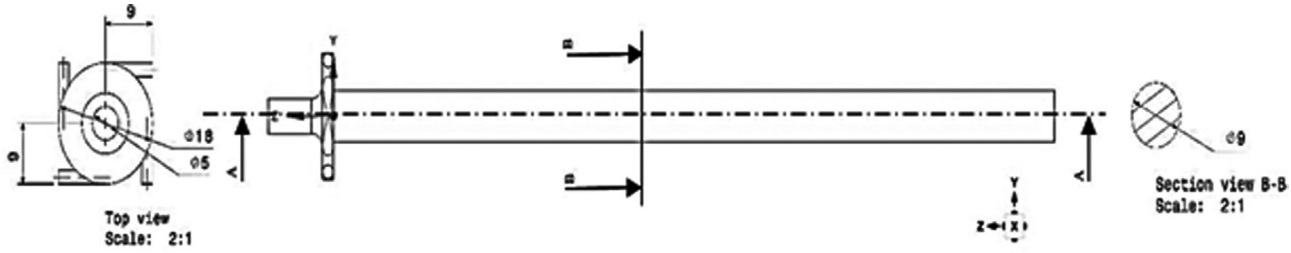

Figure 1. Diagrammatic representation of circular vortex tube.

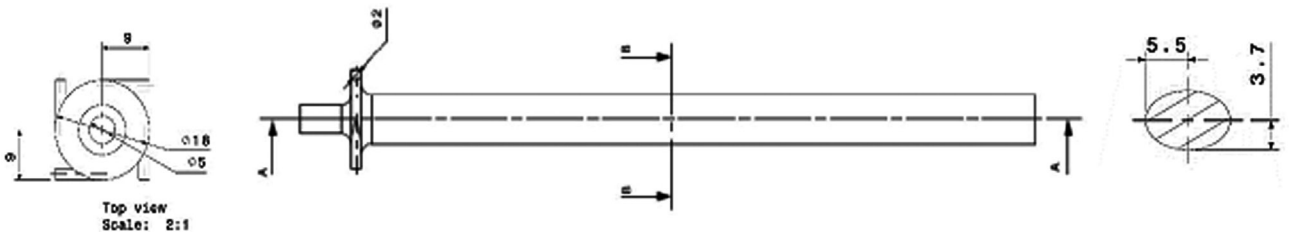

Figure 2. Diagrammatic representation of elliptical vortex tube.

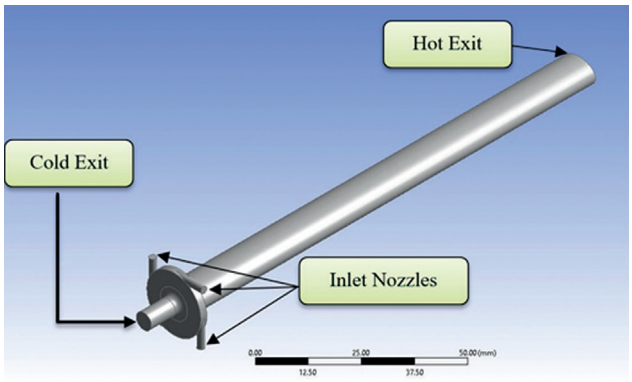

Figure 3. Computational domain of an elliptical vortex tube.

with the same cross sectional area and length as presented in Fig. 1 and 2. Table 1 contains the computational domain specifications. Here, four nozzles were used for tangentially entry of compressed air and creating turbulence inside the tube.

The computational domain was generated for the elliptical vortex tube is shown in Fig. 3. The use of FLUENT 18.2 enabled a number of simulations. In this instance, the governing equations for continuity, momentum, and energy were discretized using a solver based on pressure. To discrete the convective terms in governing equations like turbulence, energy and momentum second order upwind method has been utilised. A SIMPLE scheme had been chosen to solve the turbulence equations. The dependent variables utilized under the relaxation factor.

Governing Equations

On selecting a compressible and Newtonian fluid, air is used as the working fluid. The following are the governing equations for heat transfer and turbulent fluid flow:

- **Continuity equation**

$$\frac{\partial}{\partial x_i}(\rho u_i) = 0 \tag{1}$$

- **Momentum equation**

$$\frac{\partial \rho(u_i u_j)}{\partial x_j} = -\frac{\partial p}{\partial x_i} + \frac{\partial}{\partial x_j}\left[\mu\left(\frac{\partial u_i}{\partial x_j} + \frac{\partial u_j}{\partial x_i} - \frac{2}{3}\delta_{ij}\frac{\partial u_k}{\partial x_k}\right)\right] + \frac{\partial}{\partial x_j}(-\overline{\rho u_i' u_j'}) \tag{2}$$

- **Energy equation**

$$\frac{\partial}{\partial x_i}\left[u_i \rho\left(h + \frac{1}{2}u_i u_j\right)\right] = \frac{\partial}{\partial x_j}\left[k_{eff}\frac{\partial T}{\partial x_j} + u_i(\tau_{ij})_{eff}\right] \tag{3}$$

Further, transport equations for standard k-ε turbulence model has been equated

- **Transport Equation for *K-E* Model**

Using the following two sets of equations to solve the transport equation k- model:

$$\frac{\partial}{\partial x_i}(\rho k u_i) = \frac{\partial}{\partial x_j}\left[\left(\mu + \frac{\mu_t}{\sigma_k}\right)\frac{\partial k}{\partial x_j}\right] + G_k + G_b - \rho\varepsilon - Y_M + S_k \tag{4}$$

$$\frac{\partial}{\partial x_i}(\rho \varepsilon u_i) = \frac{\partial}{\partial x_j}\left[\left(\mu + \frac{\mu_t}{\sigma_k}\right)\frac{\partial \varepsilon}{\partial x_j}\right] + C_{1_\varepsilon}\frac{\varepsilon}{k}(G_k + C_{3_\varepsilon}G_b) - C_{2_\varepsilon}\rho\frac{\varepsilon^2}{k} + S_\varepsilon \tag{5}$$

Here,

G_k= Turbulence generation due to K.E.

G_b= Turbulence generation due to buoyancy

Y_m= Fluctuation behavior during expansion.

C_{1_ε}, C_{2_ε} & C_{3_ε} = are the constants

σ_ε and, σ_k are the Prandtl number

S_k and S_ε are the source term

These equations were discretized and solved using Fluent 18.2.

Effective Parameters

The following effective parameters to reveal the characteristics for the vortex tube. To evaluate and compared the performance of vortex tube these parameters has been utilized.

- **Pressure loss ratio**

The pressure loss ratio was evaluated in order to analyses the isentropic efficiency of elliptical and circular vortex tube. The expansion of compressible fluids is due to the pressure drop which elevate the velocity. It can be measure by the change in pressure at cold exit to the inlet pressure.

$$P_{loss} = \frac{\Delta P_{cold}}{P_{inlet}} = \frac{P_{inlet} - P_{cold}}{P_{inlet}} \tag{6}$$

The total pressure is represented by P_{inlet} (Pa) while the cold exit pressure is represented by P_{cold}.

- **Temperature difference (δt)**

The overall temperature separation can be analyse by utilising the temperature difference at the outlets. The hot and cold temperature value obtained and its difference is define as the mean temperature difference.

$$\Delta T = T_{hot} - T_{cold} \tag{7}$$

- **Cold mass fraction**

The mass flow rate is defined through the fraction of inlet and outlets. So, to replicate the experimental

procedure through a simulation the hot exit pressure varies and obtained the cold exit. The total flow remain same, therefore the amount of air entering with respect to cold exit can be varied from 0.1-0.9. This define as the rate of cold mass flow exit to the inlet mass flow rate.

$$\mu_c = \frac{\dot{m}_c}{\dot{m}_a} \tag{8}$$

Here, $\dot{m}_c$ and $\dot{m}_a$ are the mass flow rate at the cold exit and air inlet respectively.

- **Cold temperature difference**
  The difference of cold temperature with respect to the inlet show the drop in temperature inside the vortex tube.

$$\Delta T_{Cold} = T_{inlet} - T_{Cold} \tag{9}$$

Here, T_{inlet} and T_{Cold} are the temperature of the air at the inlet and cold outlet in K.

- **Isentropic efficiency**
  The vortex tube efficiency can be acquired as per adiabatic expansion of ideal gas. It is found that the expansion of air inside the tube is isentropic. Now, the energy degradation can be measure with the help of isentropic efficiency in a steady flow instruments. The actual and ideal performance of the device can be measure and compare through the isentropic efficiency parameter.

$$\eta_{isen.} = \frac{\Delta T_{cold}}{\Delta T_{isen}} = \frac{T_{inlet} - T_{Cold}}{T_{inlet}\left(1 - \frac{P_a}{P_{in}}\right)^{\frac{\gamma-1}{\gamma}}} \tag{10}$$

Boundary Conditions

The pressure conditions at the inlet and exits served to determine the boundary conditions (cold end and hot end). A 320 kPa pressure of compressed air was tangentially introduced. The observations were made while using a pressure-based implicit solver under steady state conditions. The hot exit is designated as the pressure outlet in this instance, resulting in the desired mass flow rate. By changing the pressure values at the hot pressure outlet and the cold exit, which is open to the atmosphere, the pressure values might be adjusted. A hot exit valve is used in the experimental technique to control the mass flow rate. The boundary conditions used in the current numerical analysis are kept close to those used in experiments. The pressure at the hot outlet is changed repeatedly to achieve the appropriate mass flow rate while maintaining a steady cool outlet. As a result, it met the requirements of the experiment, and numerical data were produced. Different observations, such as temperature and the cold mass fraction, are made using the experimental method at steady state. As a result, the pressure-based implicit solver has been used to run all of the simulations in a steady state condition. According to Thakare and Parekh [40], the turbulence standard k-model is valid for all cold mass fraction ranges. Therefore, the numerical solver has used a turbulence standard k-ε model with a standard wall function. Since there was a compressible and subsonic flow inside the tube, the air density model was used with air as the reference gas. By supplying the inflation close to the surfaces, the wall modelling was applied in this instance to improve the wall treatment. The chosen walls are adiabatic walls with zero heat loss and no slip. The continuity and momentum equations' convergence conditions for this numerical research were set at 10^{-4}, whereas the energy equation's default residual values were of the order of 10^{-6}.

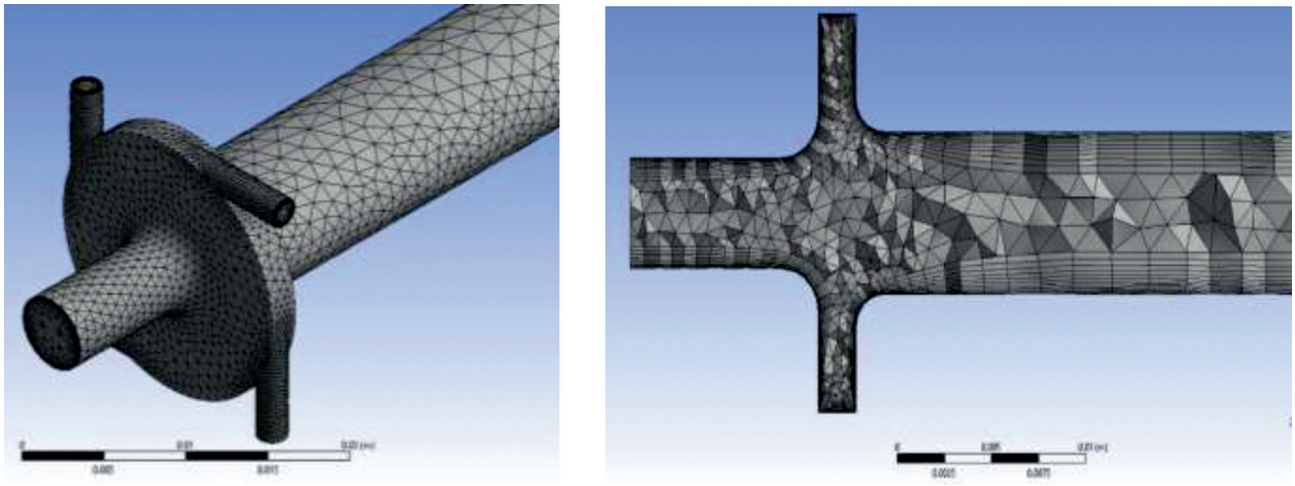

Figure 4. Grid file of generated computational domain with sectional view near the nozzle and vortex chamber of an elliptical vortex tube.

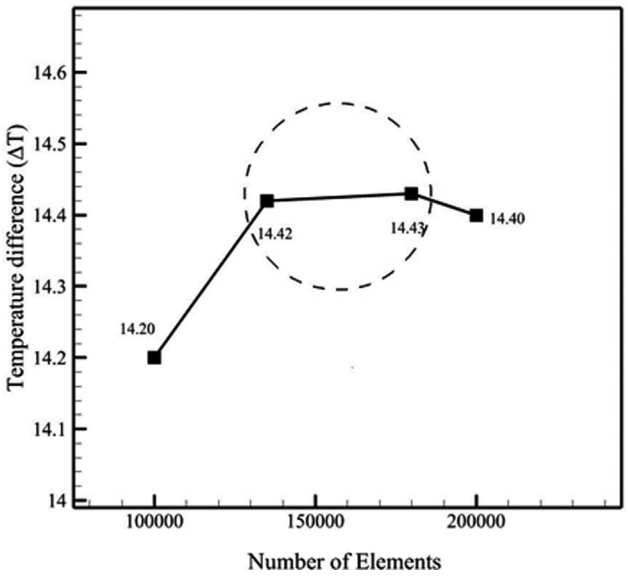

Figure 5. Variation of cold temperature to the number of elements.

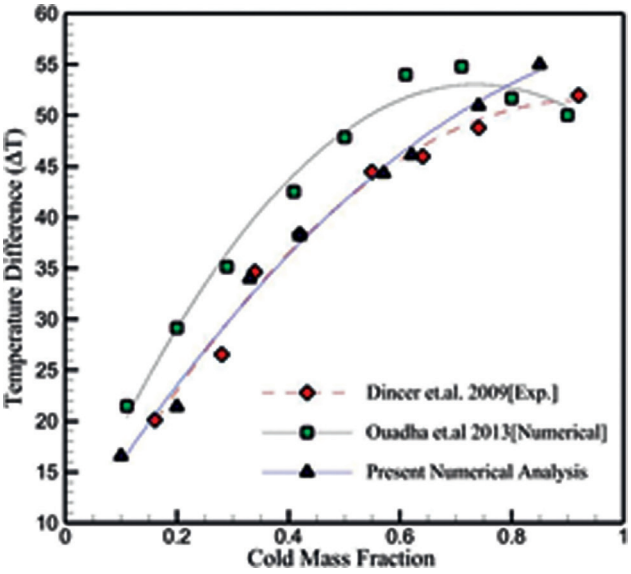

Figure 6. Temperature distribution along with cold mass fraction at 320 kPa.

Grid Independence and Validation

The errors generated due to the coarseness of the grid is an important aspect in a numerical study. To avoid these errors it is necessary to examine the grid quality. A study of the grid was conducted in the range of 1,00,000 to 2,00,000 number of elements. It is also observed how mesh density affects convergence and stability. The number of elements was 1,82,456 where the number of nodes was 80,603 has been considered for present work.

The cold exit temperatures were recorded for number of elements (1,00,000 - 2,00,000) at 0.1 cold mass fraction. Fig. 5 it is found that there is no major variation in the cold exit

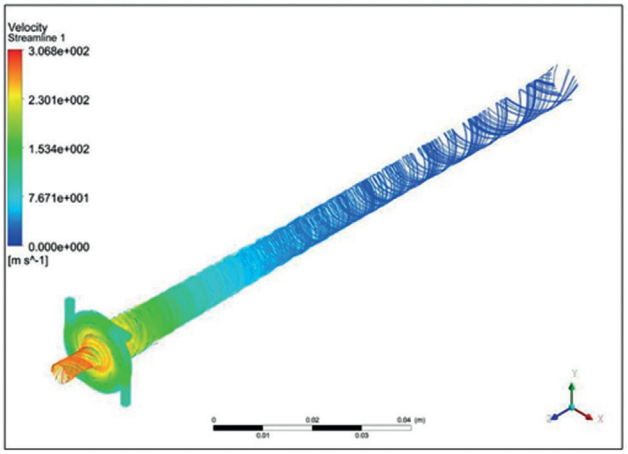

Figure 7. Streamlines of a circular vortex tube.

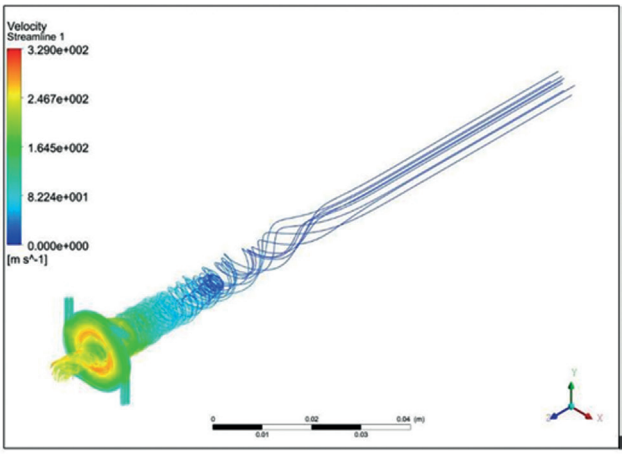

Figure 8. Streamlines of an elliptical vortex tube.

temperature values beyond 1,80,000 elements. Hence, it is assumed that the remaining study can be carried out with this number of elements

The mean temperature difference is obtained through numerical analysis and is compared as shown in Fig. 6. Both the researcher Ouadha et al. [39] and Dincer et al. [41] computed their results in the form of the mean temperature of hot and cold stream at various μ_c and pressure inlet. The graph shows that the numerical results for mean temperature are similar to those of Ouadha et al. [39] and Dincer et al. [41]. The reason of deviation may be due to the different environmental conditions. Further, present study has been made considering air as an ideal gas with smooth surface considering no slip adiabatic conditions.

RESULTS AND DISCUSSION

The numerical investigation has been conducted utilizing CFD to explore the flow characteristics and temperature

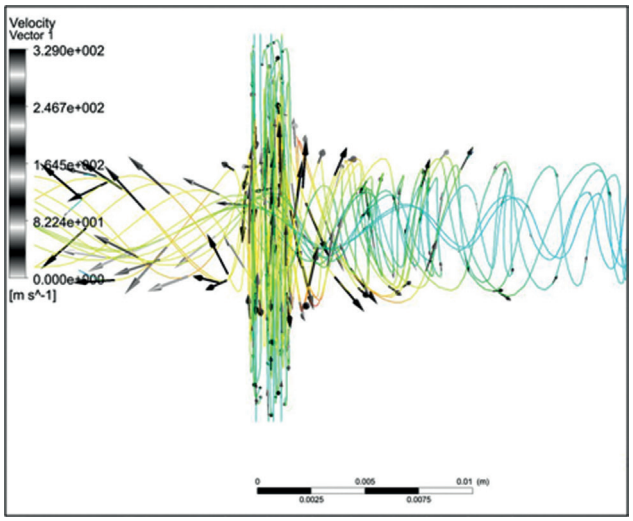

Figure 9. Streamline and vector representation of flow pattern of vortex chamber of circular vortex tube.

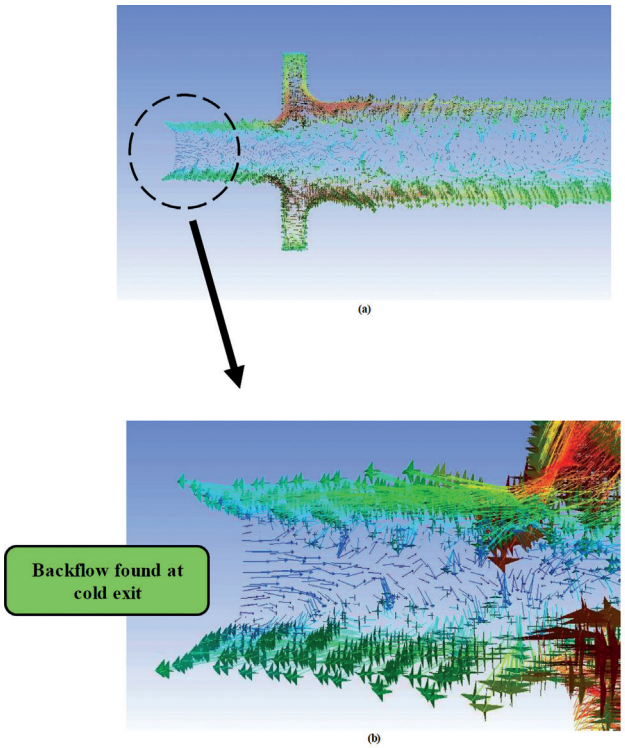

Figure 10. (a) Vector representation of flow pattern near the cold exit in an elliptical vortex tube for low cold mass fraction (b) Enlarge view of cold exit showing backflow.

separation effect inside an elliptical vortex tube. The influence of elliptical shape over the performance of vortex tube also discussed and compared with circular vortex tube. To evaluate the performance the difference between the mean temperature values of hot and cold exit for both the vortex tubes are taken. Also, the isentropic efficiency has been reported for various pressure loss ratio. The flow pattern inside an elliptical and circular vortex tube are shown via velocity contours and streamline contours. Fig. 7 and 8 represents the three dimensional streamlines for both the circular and elliptical vortex tube respectively evaluated through standard k-ε turbulence model for 320 kPa inlet pressure. It is detected that the energy separation in both the vortex tubes is because of high-rotational flow. The cause of high-rotational flow is due to the angular momentum transfer from centre to the end of the tube. The velocity is maximum at the cold exit where as it decreases as it transfers close to the peripheral of the hot stream. This defines the existence of high turbulence in both the vortex tubes as shown in Fig. 7 and 8.

The velocity vector represents the direction of swirling flow inside the tubes as shown in Fig. 9 and 10. This illustrate the accurate flow physics and validate the methodology proposed in present work. The backflow of atmospheric air is originate at the cold exit as showing in Fig. 10 (b) which influence the temperature separation. This temperature separation magnitude is largely affected by the backflow of the atmospheric air at low cold mass fraction values. Furthermore, as the value of cold mass fraction increases the backflow dissipated.

- **Velocity Components and Flow Field**

The axial and tangential velocity contours indicates that the maximum velocity was at the cold peripheral as the tube length increases, the velocity also drops at the hot outlet of the vortex tube. For the total pressures of 320 kPa, the maximum tangential velocity is 324 m/s and 276 m/s in an elliptical vortex tube and circular vortex tube respectively. In an elliptical vortex tube the tangential velocity is high as compared to circular vortex tube that may be the reason of high temperature separation in an elliptical vortex tube. The maximum velocity is found near the inlet wall where cold exit is located which shows the presence of high kinetic energy. Moreover, the magnitude of low velocity at the hot stream peripheral represents a lower magnitude of kinetic energy. Due to the abrupt expansion of air near the axis, the increased axial velocity progressively increases in the negative area. The contour of axial velocity also justify that the highest flow rate is achieved near the inlet and cold exit peripheral as shown in Fig. 11 and 12. The axial velocity keeps on decreasing as it displaces near to the hot stream. A lower degree of axial velocity is found as compared to tangential velocity. Moreover, in both cases, fluid velocity diminished while it reaches the end of the hot exit. The axial velocity decelerated to a minimum value for a particular position of tube radius. Here, the positive and negative values indicates the hot and cold regions inside the tube as shown in Fig. 13.

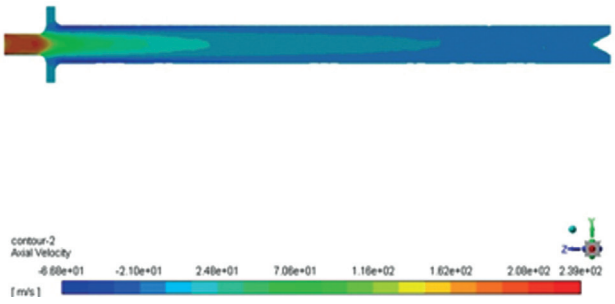

Figure 11. Axial velocity contour of a circular vortex tube.

Figure 12. Axial velocity contour of an elliptical vortex tube.

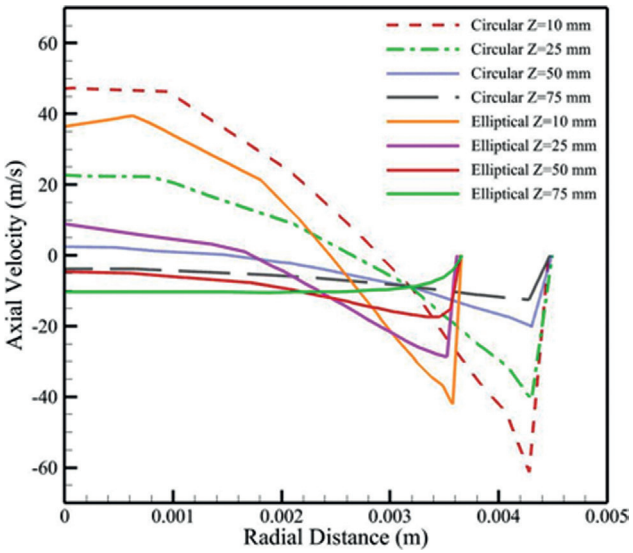

Figure 13. Axial velocity comparison of circular and elliptical vortex tube.

Figure 14. Tangential velocity contour of a circular vortex tube.

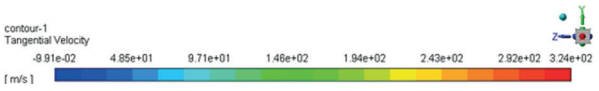

Figure 15. Tangential velocity contour of an elliptical vortex tube.

It is worth noting that the decrement of axial velocity in an elliptical vortex tube is less as compared to circular vortex tube. The effect is may be due to its elliptical shape in which molecular momentum is high. In Fig. 14 and 15, the swirl or tangential velocity is shown, and it can be observed that it is much higher than axial velocity and dominates the flow. In both cases, at the vortex tube's surface, the tangential shear stress gradually developed the elevation towards the end of the tube. The tangential velocity drops at the surface of the vortex tube and increases in the radial direction. While comparing with the circular vortex tube, the flow shows similar trends but has a substantial difference in values observed during the investigation. It is found that the swirl flow generates the forced vortex at the maximum region inside the tube and free vortex towards the wall of the tube.

In relation to radial distance, Figs. 13 and 16 demonstrate the comparative analysis of axial velocity and tangential velocity for the two geometries. The positions of longitudinal length are Z=10, 25, 50, 75 mm. The velocity drops because of free vortex is generated close to the wall and extended to stagnation point at the centre of the tube. In the centre of the tube working fluid moves with a dropped kinetic energy where the tangential velocity is low. It can be suggested from the analysis that the temperature separation effects are dominating by the rotational flow of the compressed air. The energy transfer takes place due to angular momentum transfer. The flow moves towards the core to peripheral define the presence of turbulence generated through an angular momentum shown in Fig. 14

and 15. The graphical representation of tangential velocity inside the tube also satisfy the flow physics as shown in Fig. 16. The temperature increases due to the energy transformation, which was developed through kinetic energy. Also, the temperature dropped due to the pressure growth and angular momentum transfer at the tube's surface.

- **Influence of Density and Pressure**

Fig. 17 and 18 indicates the flow pattern of density and total pressure. The total pressure and density contour matches the trend in both the vortex tubes. The elliptical vortex tube achieved the maximum value of density and total pressure as compared to circular shape. The significant centrifugal force created by the high density differential inside the tube is the primary source of temperature separation. It is obvious that this inconsistency in the density gradient caused the energy separation.

The static pressure inside the tube varies depending on the radial distance, as shown in Fig. 21. The graphical representation demonstrates that the hot end is where the pressure gradient is lowest and where the largest static pressure is located. The sudden air expansion, friction, and flow resistance with the wall are the likely causes of this. The tube's end experiences a decrease in pressure due to the resistive force. The abrupt rises and drops in velocity at the wall surfaces are also depicted in Fig. 22. Comparing a circular vortex tube to an elliptical one, the circular velocity magnitude is greater.

- **Temperature Distribution**

The temperature separation phenomena inside the vortex tube was proposed by many researchers. Xue et al. [42] thoroughly explained the temperature or energy separation phenomena inside the vortex tube. The study explained the

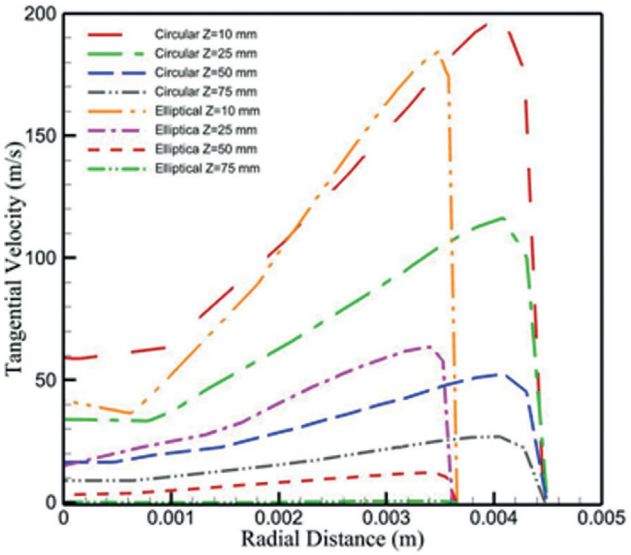

Figure 16. Tangential velocity comparison of circular and elliptical vortex tube.

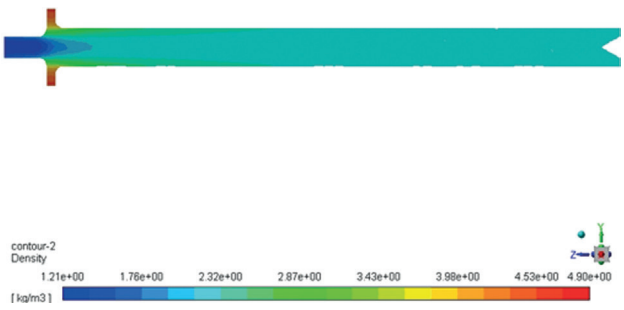

Figure 17. Density contour of a circular vortex tube.

Figure 18. Density Contour of an elliptical vortex tube.

Figure 19. Variation of total pressure inside a circular vortex tube.

Figure 20. Variation of total pressure inside an elliptical vortex tube.

number of factors caused the temperature separation. The cause of temperature separation included pressure gradient inside the tube, friction between the working fluid and the walls of the vortex tube, the high turbulence air entering the system, also the static temperature difference, secondary circulation and acoustic streaming. Figures 23 to 28 depict the static and overall temperature distributions for both vortex tubes. The total temperatures for the elliptical and circular vortex tubes are 316 K and 312 K, respectively, and 249 K and 246 K, respectively. Low kinetic energy is the cause of the overall temperature increasing at the tube's end and decreasing at the cold end. The static temperature variation for both vortex tubes with regard to radial

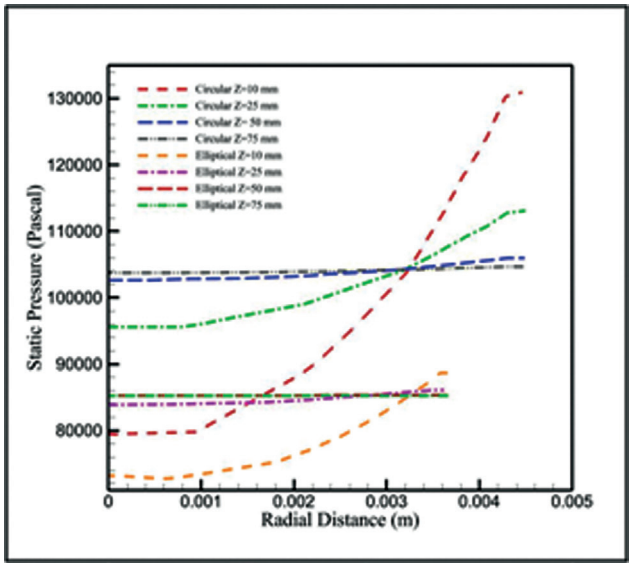

Figure 21. Static pressure comparison of circular and elliptical vortex tube.

Figure 23. Variation of static temperature inside the circular vortex tube.

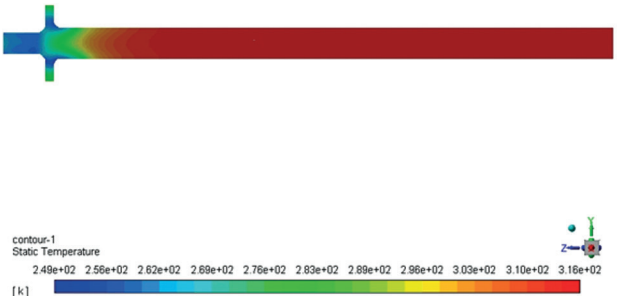

Figure 24. Variation of static temperature inside an elliptical vortex tube.

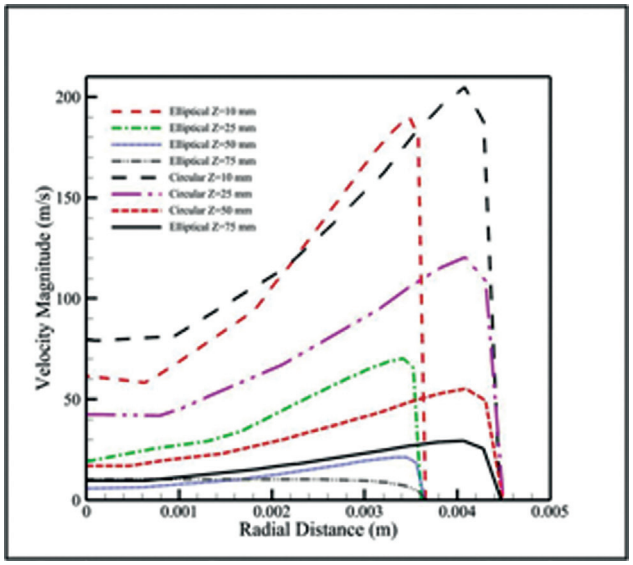

Figure 22. Velocity magnitude of comparison of circular and elliptical vortex tube.

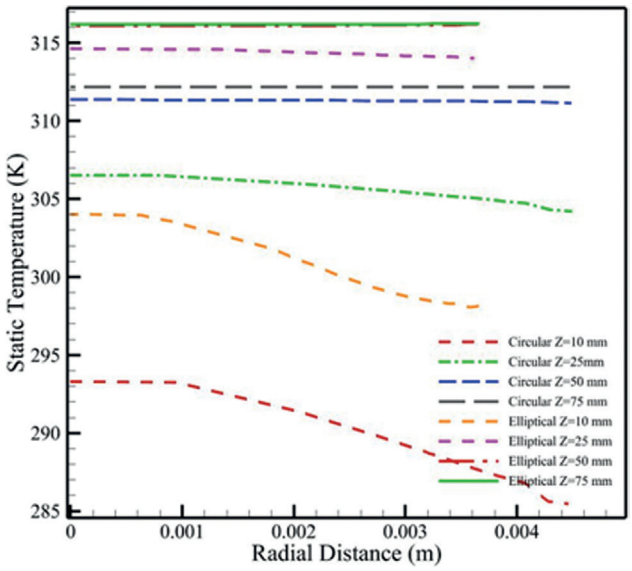

Figure 25. Static Temperature comparison of circular and elliptical vortex tube.

direction was shown in Fig. 25. As the flow moves closer to the tube wall, the static temperature suddenly drops, as seen on the graph. The rapid increase of air near the inlet wall is to the cause for the decrease in static temperature. Such growth of air reports high swirl velocity which drops the static temperature.

The overall temperature in the radial direction for both vortex tubes is compared in Fig. 28. The swirling flow effect inside the tubes is created by the highly compressed air's immense kinetic energy. It has been found that the temperature separation effect developed as a result of radial pressure and kinetic energy. The comparison between turbulent kinetic energy and overall temperature was also established. The Fig. 29 clearly shows that the elliptical vortex tube had the maximum turbulent kinetic energy, whereas the circular vortex tube had the lowest. The sudden expansion of air as it moved from the tube's axial centre layer to the wall caused the kinetic energy and overall temperature to drop. The thermal energy is obtained by the air particles when they expand longitudinally close to the hot exit. Here, when the velocity decreases, the shear effect converts the kinetic energy into thermal energy, causing the static temperature to grow throughout the longitudinal length.

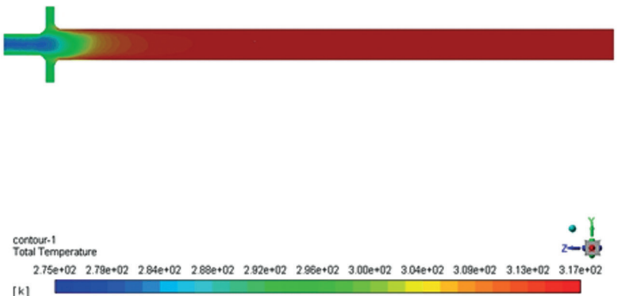

Figure 27. Variation of total temperature of an elliptical vortex tube.

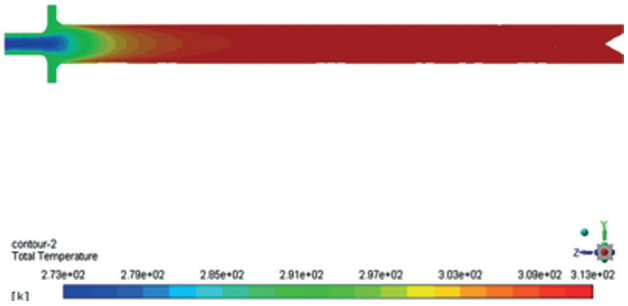

Figure 26. Variation of total temperature inside a circular vortex tube.

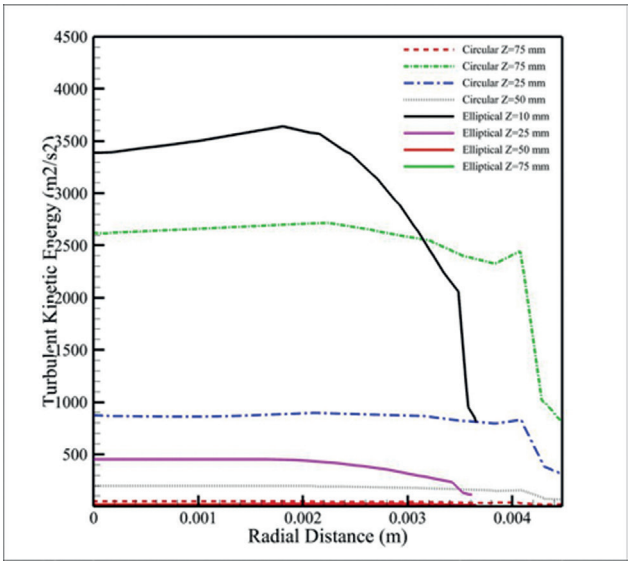

Figure 29. Turbulent K.E. comparison of circular and elliptical vortex tube.

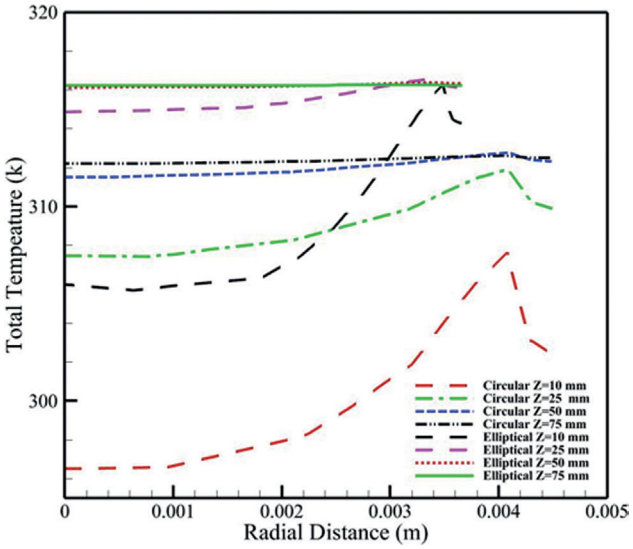

Figure 28. Total temperature comparison of circular and elliptical vortex tube.

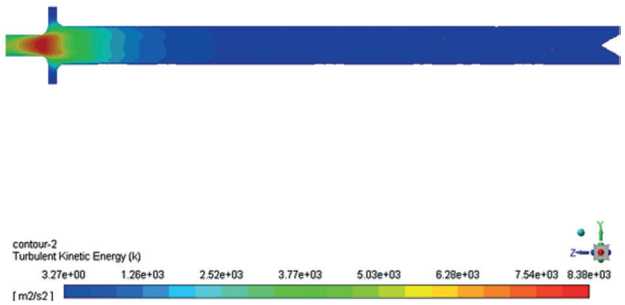

Figure 30. Turbulent kinetic energy contour of a circular vortex tube.

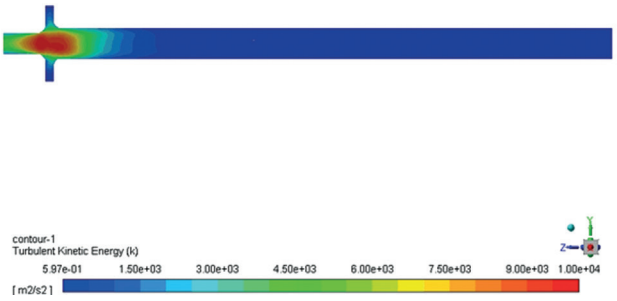

Figure 31. Turbulent kinetic energy contour of an elliptical vortex tube.

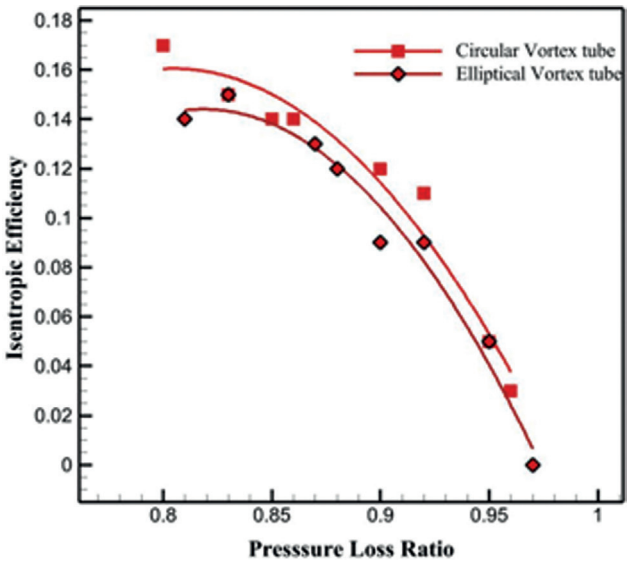

Figure 32. Performance of elliptical and circular vortex tube on the bases of isentropic efficiency along with Pressure drop.

- **Performance**

Fig. 32 shows the variation between isentropic efficiency and pressure loss ratio, as the pressure loss ratio increases the efficiency decreases. The isentropic efficiency was obtained at the pressure loss ratio of 0.8 to 1. The isentropic efficiencies are 0.14 and 0.17 for elliptical and circular vortex tube respectively at 0.81 pressure loss ratio. In elliptical vortex tube the isentropic efficiency is less as compared to the circular vortex tube for the same pressure loss ratio. Despite that the temperature separation in an elliptical vortex tube is substantial high at low cold fraction and it quiet near for high cold mass fraction. It is found that energy separation in an elliptical tube is increased by 49.89% at hot end and 22.65% at cold end as compared to circular tube at 0.2 μ_c. A significant temperature rise can be observed in the elliptical model. An elliptical hot tube

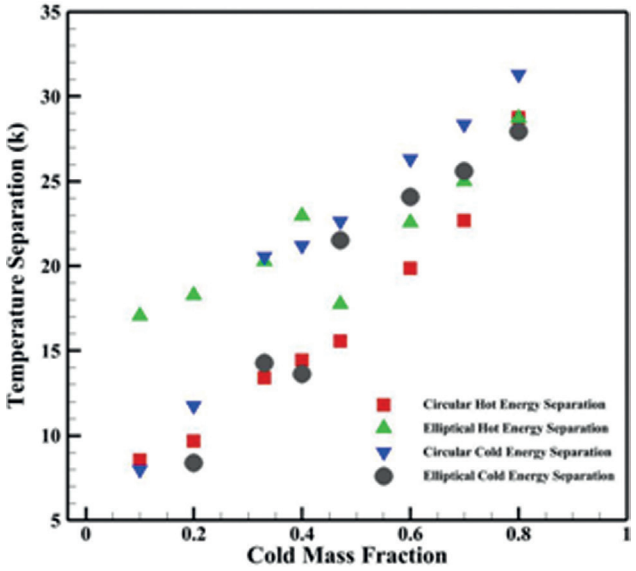

Figure 33. Temperature Separation with respect to cold mass fraction.

expands the compressed air with high turbulent eddies to generates energy separation.

CONCLUSION

In this work, a CFD approach was carried out to examine the flow mechanism and energy separation in an elliptical vortex tube and compared with the circular vortex tube. The significance of the work are summarized as follows:

- The mean kinetic energy moves with high velocity generates the diffusion inside the vortex tube. This diffusion creates the temperature separation effect. Furthermore, the temperature separation effect and diffusion also influenced by various parameters like inlet pressure, mass flow rate, pipe length and shapes. The study also discussed the reason behind the high velocity at the core and low velocity at the peripheral of hot tube. The present work also illustrates a reasonable justification for the temperature difference and flow physics inside an elliptical tube.
- The exchange of energy between kinetic energy and angular momentum that produces the turbulence dominates the flow and causes the temperature difference inside the tube.
- The work also illustrate the temperature separation effect concerning its shape and length. It is observed that the temperature separation can be improved by changing its shape until critical tube length. The elliptical shape generates high-temperature distributions as compared to circular with the same area and other specifications. In both geometries, the vortex tube's centre has a high velocity and pressure that decreases as the air moves towards the heated outlet.

- It can be observed that the elliptical model's efficiency is less as compared to the circular vortex tube, but the energy separation is relatively higher.

NOMENCLATURE

3D	Three Dimension
ANN	Artificial neural network
CFD	Computational Fluid Dynamics
L	Tube length, mm
D	Diameter of vortex tube, mm
μ_c	Cold mass fraction
COP	Coefficient of performance
L_{tube}	hot tube length , mm
D_{inlet}	diameter of inlet, mm
H_{nozzle}	height of nozzle, mm
W_{nozzle}	Width of nozzle, mm
D_{cold}	Cold orifice diameter, mm
$A_{hot\ tube}$	Area of hot tube, mm^2
ΔT_{cold}	Temperature separation at cold outlet, K
P_{inlet}	Inlet pressure , kPa
P_{cold}	Pressure at cold exit, kPa
k	Thermal conductivity $Wm^{-1}K^{-1}$
u	Mass-aveaged velocity ms^{-1}
u'	Fluctuating velocity component ms^{-1}
x	x-coordinate
δ_{ij}	Kronecker delta
ε	Turbulence dissipation rate $m^2\ s^{-3}$
ρ	Density kg m^{-3}
τ	Stress tensor Pa

Greek alphabets

$\eta_{isentropic}$	Isentropic efficiency
ρ	Fluid density,kgm^{-3}
α	Thermal diffusivity, m^2s^{-1}
γ	Adiabatic constant

Subscript

Inlet	Inlet region
cold	Cold outlet
hot	Hot outlet
eff	Effective
i,j,k	Cartesian indices

ACKNOWLEDGMENT

The author would like to appreciatively acknowledge the provision of Dr. Hitesh Thakare and Dr. Aniket Monde for valuable discussion on this study.

AUTHORSHIP CONTRIBUTIONS

Authors equally contributed to this work.

DATA AVAILABILITY STATEMENT

The authors confirm that the data that supports the findings of this study are available within the article. Raw data that support the finding of this study are available from the corresponding author, upon reasonable request.

CONFLICT OF INTEREST

The author declared no potential conflicts of interest with respect to the research, authorship, and/or publication of this article.

ETHICS

There are no ethical issues with the publication of this manuscript.

REFERENCES

[1] Markal B, Aydin O, Avci M. An experimental study on the effect of the valve angle of counter-flow Ranque-Hilsch vortex tubes on thermal energy separation. Exp Therm Fluid Sci 2010;34:966–971. [CrossRef]

[2] Kirmaci V, Uluer O. The effects of orifice nozzle number on heating and cooling performance of vortex tubes: An experimental study. Instrum Sci Technol 2008;36:493–502. [CrossRef]

[3] Krmaci V, Uluer O, Dincer K. An experimental investigation of performance and exergy analysis of a counterflow vortex tube having various nozzle numbers at different inlet pressures of air, oxygen, nitrogen, and argon. J Heat Transfer 2010;132:121701. [CrossRef]

[4] Rafiee SE. Sadeghiazad MM. Three-dimensional and experimental investigation on the effect of cone length of throttle valve on thermal performance of a vortex tube using k-ε turbulence model. Appl Therm Eng 2014;66:65–74. [CrossRef]

[5] Gutak AD. Experimental investigation and industrial application of Ranque-Hilsch vortex tube. Int J Refrig 2015;49:93–98. [CrossRef]

[6] Li N, Zeng ZY, Wang Z, Han XH, Chen GM. Experimental study of the energy separation in a vortex tube. Int J Refrig 2015;55:93–101. [CrossRef]

[7] Senturk Acar M, Arslan O. Exergo-economic Evaluation of a new drying system Boosted by Ranque-Hilsch vortex tube. Appl Therm Eng 2017;124:1–16. [CrossRef]

[8] Nouri-Borujerdi A, Bovand M, Rashidi S, Dincer K. Geometric parameters and response surface methodology on cooling performance of vortex tubes. Int J Sustain Energy 2017;36:872–886. [CrossRef]

[9] Yadav BUM, Reddy GMP, Gowd PM. Effect of end control plugs on the performance of vortex tube with dual forced vortex flow. J Therm Eng 2016;2:871–881. [CrossRef]

[10] Westley R. A bibliography and survey of vortex tube. Coll Aeronaut Cranf 1954:39. https://dspace.

lib.cranfield.ac.uk/bitstream/handle/1826/11120/COA_N_9_1954.pdf?sequence=1. Last Accessed Date: 07.03.2023.

[11] Kurosaka M. Acoustic streaming in swirling flow and the Ranque-Hilsch (vortex-tube) effect. J Fluid Mech 1982;124:139–172. [CrossRef]

[12] Uluer O, Kirmaci V, Atas S. Using the artificial neural network model for modeling the performance of the counter flow vortex tube. Expert Syst Appl 2009;36:12256–12263. [CrossRef]

[13] Eiamsa-ard S, Promvonge P. Review of Ranque-Hilsch effects in vortex tubes. Renew Sustain Energy Rev 2008;12:1822–1842. [CrossRef]

[14] Ahlborn BK, Gordon JM. The vortex tube as a classic thermodynamic refrigeration cycle. J Appl Phys 2000;88:3645–3653. [CrossRef]

[15] Behera U, Paul PJ, Kasthurirengan S, Karunanithi R, Ram SN, Dinesh K, et al. CFD analysis and experimental investigations towards optimizing the parameters of Ranque-Hilsch vortex tube. Int J Heat Mass Transf 2005;48:1961–1973. [CrossRef]

[16] Aljuwayhel NF, Nellis GF, Klein SA. Parametric and internal study of the vortex tube using a CFD model. Int J Refrig 2005;28:442–450. [CrossRef]

[17] Skye HM, Nellis GF, Klein SA. Comparison of CFD analysis to empirical data in a commercial vortex tube. Int J Refrig 2006;29:71–80. [CrossRef]

[18] Farouk T, Farouk B. Large eddy simulations of the flow field and temperature separation in the Ranque-Hilsch vortex tube. Int J Heat Mass Transf 2007;50:4724–4735. [CrossRef]

[19] Xue Y, Arjomandi M, Kelso R. Energy analysis within a vortex tube. Exp Therm Fluid Sci 2014;52:139–145. [CrossRef]

[20] Rahimi M, Rafiee SE, Pourmahmoud N. Numerical investigation of the effect of divergent hot tube on the energy separation in a vortex tube. Int J Heat Technol 2013;31:17–26. [CrossRef]

[21] Pourmahmoud N, Esmaily R, Hassanzadeh A. Experimental investigation of diameter of cold end orifice effect in vortex tube. J Thermophys Heat Transf 2015;29:629–632. [CrossRef]

[22] Agrawal N, Naik SS, Gawale YP. Experimental investigation of vortex tube using natural substances. Int Commun Heat Mass Transf 2014;52:51–55. [CrossRef]

[23] Bazgir A, Nabhani N. Investigation of temperature separation inside various models of Ranque-Hilsch vortex tube: Convergent, straight, and divergent with the help of computational fluid dynamic approach. J Therm Sci Eng Appl 2018;10:051013. [CrossRef]

[24] Rafiee SE, Sadeghiazad MM. Experimental and CFD analysis on thermal performance of Double-Circuit vortex tube (DCVT)-geometrical optimization, energy transfer and flow structural analysis. Appl Therm Eng 2018;128:1223–1237. [CrossRef]

[25] Pourmahmoud N, Rashidzadeh M, Hassanzadeh A. CFD investigation of inlet pressure effects on the energy separation in a vortex tube with convergent nozzles. Eng Comput 2015;32:1323–1342. [CrossRef]

[26] Rafiee SE, Sadeghiazad MM, Mostafavinia N. Experimental and numerical investigation on effect of convergent angle and cold orifice diameter on thermal performance of convergent vortex tube. J Therm Sci Eng Appl 2015;7:041006. [CrossRef]

[27] Zangana LMK, Barwari RRI. The effect of convergent-divergent tube on the cooling capacity of vortex tube: An experimental and numerical study. Alex Eng J 2020;59:239–246. [CrossRef]

[28] Bovand M, Valipour MS, Dincer K, Tamayol A. Numerical analysis of the curvature effects on Ranque-Hilsch vortex tube refrigerators. Appl Therm Eng 2014;65:176–183. [CrossRef]

[29] Bazgir A, Nabhani N, Eiamsa-ard S. Numerical analysis of flow and thermal patterns in a double-pipe Ranque-Hilsch vortex tube: Influence of cooling a hot-tube. Appl Therm Eng 2018;144:181–208. [CrossRef]

[30] Thakare HR, Parekh AD. Experimental investigation of Ranque — Hilsch vortex tube and techno – Economical evaluation of its industrial utility. Appl Therm Eng 2020;169:114934. [CrossRef]

[31] Reddy PS, Sreedevi P. Effect of thermal radiation and volume fraction on carbon nanotubes based nanofluid flow inside a square chamber. Alexandria Eng J 2021;60:1807–1817. [CrossRef]

[32] Sreedevi P, Reddy PS. Heat and mass transfer analysis of MWCNT-kerosene nanofluid flow over a wedge with thermal radiation. Heat Transf 2021;50:10–33. [CrossRef]

[33] Sreedevi P, Reddy PS. Impact of convective boundary condition on heat and mass transfer of nanofluid flow over a thin needle filled with carbon nanotubes. J Nanofluids 2020;9:282–292. [CrossRef]

[34] Sreedevi P, Reddy PS. Entropy generation and heat transfer analysis of alumina and carbon nanotubes based hybrid nanofluid inside a cavity. Phys Scr 2021;96:085210. [CrossRef]

[35] Sreedevi P, Reddy PS. Effect of SWCNTs and MWCNTs Maxwell MHD nanofluid flow between two stretchable rotating disks under convective boundary conditions. Heat Transf Asian Res 2019;48:4105–4132. [CrossRef]

[36] Sreedevi P, Reddy PS, Chamkha AJ. Magnetohydrodynamics heat and mass transfer analysis of single and multi-wall carbon nanotubes over vertical cone with convective boundary condition. Int J Mech Sci 2018;135:646–655. [CrossRef]

[37] Reddy PS, Sreedevi P, Chamkha AJ. Heat and mass transfer flow of a nanofluid over an inclined plate under enhanced boundary conditions with

magnetic field and thermal radiation. Heat Transf Asian Res 2017;46:815–839. [CrossRef]

[38] Sudarsana Reddy P, Jyothi K, Suryanarayana Reddy M. Flow and heat transfer analysis of carbon nanotubes-based Maxwell nanofluid flow driven by rotating stretchable disks with thermal radiation. J Brazilian Soc Mech Sci Eng 2018;40:1–16. [CrossRef]

[39] Ouadha A, Baghdad M, Addad Y. Effects of variable thermophysical properties on flow and energy separation in a vortex tube. Int J Refrig 2013;36:2426–2437. [CrossRef]

[40] Thakare HR, Parekh AD. Computational analysis of energy separation in counter-flow vortex tube. Energy 2015;85:62–77. [CrossRef]

[41] Dincer K, Baskaya S, Uysal BZ, Ucgul I. Experimental investigation of the performance of a Ranque-Hilsch vortex tube with regard to a plug located at the hot outlet. Int J Refrig 2009;32:87–94. [CrossRef]

[42] Xue Y, Arjomandi M, Kelso R. A critical review of temperature separation in a vortex tube. Exp Therm Fluid Sci 2010;34:1367–1374. [CrossRef]